treatment with AFCA-B-P-(SN-38)$_3$ was a change in gross tumor color from reddish to white (Fig. 3C). To clarify the cause for this change in color, the histopathological features of the tumor stroma after immunoconjugate therapy were examined. There was no clear change in fibroblasts or macrophages, which play an important role in tumor progression[31,32] (data not shown). We then evaluated stromal vascular changes both qualitatively and quantitatively using immunohistochemistry and *in vivo* fluorescence endomicroscopy. Using these techniques, discontinuation and irregularity comprising a mixture of narrowness and enlargement of tumor vessels were manifested following treatment with AFCA-B-P-(SN-38)$_3$ (Fig. 3D,E).

Discussion

It is known that LMW ACA, including molecular targeting agents, can easily extravasate from normal blood vessels, resulting in various adverse effects (Fig. 4A). To overcome the off-target effects caused by LMW ACA, an immunoconjugate therapy was developed in which ACA or a toxin is conjugated to a cancer cell-specific mAb (Fig. 4B).

The immunoconjugates selectively extravagate from leaky tumor vessels and this is an advantage in cancer treatment. However, to date, immunoconjugate therapies for common solid tumors have not been successful in clinical practice because of the heterogeneity of the target antigens.[1–6,8,9] Moreover, most human tumors have abundant stroma that hinders the distribution of the immunoconjugate. Our basic strategy for overcoming the stromal barrier as a protective shield for cancer cells is to make use of the fibrin in the stroma as a scaffold assembly of the immunoconjugates, followed by the release of SN-38 to the cancer cells. This free SN-38 can easily reach the cancer cells by diffusion through the stromal barrier. Another important finding of the present study is that SN-38 released from the immunoconjugates and located in the fibrin networks around the tumor vasculature may attack vascular endothelial cells.

During the process of blood coagulation, extrinsically activated thrombin cleaves fibrinopeptides A and B from the α- and β-chains of fibrinogens, generating soluble fibrin monomers. Thereafter, an insoluble fibrin clot forms following enzymatic and non-enzymatic processing.[33] Therefore, it is speculated that the epitope of our anti-fibrin mAb is adjacent to the thrombin cutting site of the fibrinogens.

Another feature of our anti-fibrin mAb is the conversion of human chimeric IgG from mouse IgM using an antibody engineering technique. The use of human chimeras is beneficial for clinical applications to avoid human anti-mouse neutralizing antibodies and allergic reactions in humans. In addition, because of the rapid blood clearance and low penetration of IgM compared with IgG, based on the faster elimination of IgM from the liver and its larger molecular size,[34] IgM is not suitable as a drug delivery vehicle.

The anti-fibrin mAb was conjugated with SN-38 using newly designed linker assembly. SN-38 is a topoisomerase I inhibitor, with time-dependent antitumor activity, and is an active component of CPT-11, which is used clinically in the treatment of

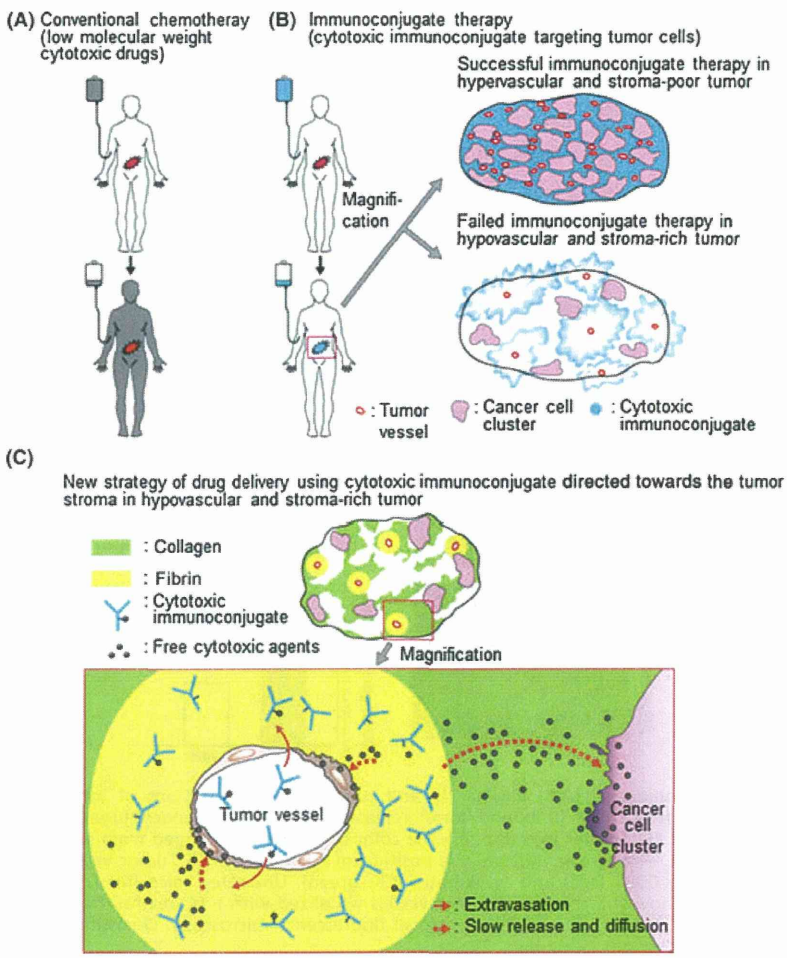

Fig. 4. Diagram of the background and the new concept of drug delivery using tumor stroma as a ligand. (A) Low molecular weight anticancer agents (black) can be distributed throughout the entire body, resulting in serious side effects. (B) Cytotoxic immunoconjugates (blue) accumulate selectively in the tumor tissue. Successful (upper) and failed (lower) immunoconjugate therapy is shown. (C) The newly developed immunoconjugate (i.e. anti-fibrin chimeric IgG–branched-PEG-(SN-38)$_3$) extravasates selectively from leaky tumor vessels, binds specifically to the fibrin network around the tumor vessels to create a scaffold, and then allows the effective, sustained release of SN-38, an anticancer agent with time-dependent effects, from the scaffold. Because this released anticancer agent is of a low molecular weight, it is subsequently distributed throughout the entire tumor stroma, which normally acts as a barrier, and induces damage not only to tumor cells, but also to tumor vessels.

doi: 10.1111/j.1349-7006.2011.01954.x

colorectal, lung, and other cancers.[35] Linker technology is an important part of immunoconjugate chemotherapy, and various linkers have been exploited to date. Of these, acid labile hydrazone linkage, thiol reduction of disulfide linkers, and enzymatic proteolysis of peptide linkers have been used successfully to ensure stability in plasma.[26–28] For these types of linkers, cell-mediated endocytosis and intracellular processing of the immunoconjugates are indispensable to make the active agent work. In our newly deployed linker construct, an ester bond can release SN-38 gradually, independent of enzymes, under physiological conditions such as in the extracellular environment. In our design, PEG was combined close to this ester bond. It is known that PEG evades non-specific capture by the reticuloendothelial system (RES) in the body, with the steric structure around the bond protecting against immunoconjugate degradation in the blood. Furthermore, PEG has already been used for this purpose.[11,12] Moreover, the unique branched composition enables the attachment of three SN-38 molecules, rather than only one as in standard linear types of linkers.

As mentioned above, asymptomatic fibrin formation occurs only during cancer invasion and metastasis. Patients with advanced cancer are candidates for treatment with systemic ACA and almost all such patients are fibrin free, except for in the cancer tissue in the body. In addition, HMW proteins, including IgG, cannot extravasate from normal blood vessels to cause unwanted side effects in non-neoplastic organs (Fig. 4C). In spontaneous mouse tumors characterized by abundant stroma, this cancer stroma-targeting therapy using tumor-induced fibrin clots has succeeded, for the first time, in producing conditions that achieve drug exposure levels specifically in tumor cells that are similar to those in monolayer culture dishes and it is thus a highly effective new strategy for treating solid tumors, especially stroma-rich cancers, which are refractory to conventional therapy. In the 1960s, and ^{131}I-Ab that targeted fibrin was suggested as a potential cancer therapy.[36] However, that Ab was polyclonal and reacted with fibrinogen, which is the physiological precursor of fibrin and abundant in the blood stream. The polyclonal Ab against fibrin bound to fibrinogen in the blood stream and easily changed to a circulating immune complex. This immune complex was eliminated more rapidly from the liver than intact IgG, resulting in rapid blood clearance.[34,37] In fact, the present study demonstrated that the accumulation of the anti-fibrinogen mAb was weaker and that the anti-fibrinogen mAb was eliminated more rapidly than the anti-fibrin chimeric mAb.

This linker technology can be applied to many other ACA, including molecular targeting agents. Thus, this present discovery, the development of which was based on cancer pathophysiology and organic chemistry, may change current therapy with ACA and open a new fields of medical science, consequently producing many useful treatment modalities in the field of oncology, cardiovascular disease, and inflammation.

Acknowledgments

This work was supported by the Third Term Comprehensive Control Research for Cancer from the Ministry of Health, Labour and Welfare of Japan (YM), a Grant-in-Aid for Scientific Research on Priority Areas from the Ministry of Education, Culture, Sports, Science and Technology, the Princess Takamatsu Cancer Research Fund (YM), the Japanese Foundation for Multidisciplinary Treatment of Cancer (YM), and a Grant-in-Aid for Scientific Research from Japan Society for the Promotion of Science (MY). The authors thank Drs. D Tarin (Department of Pathology, University of California, La Jolla, San Deigo, CA, USA), J Kuroda (Investigative Treatment Division, Research Center for Innovative Oncology, National Cancer Center Hospital East, Kashiwa, Japan), and T Sugino (Department of Basic Pathology, Fukushima Medical University, Fukushima, Japan) for their helpful discussions. The authors also thank Mrs. H Koike and Mrs. M Mizoguchi-Araake for their technical assistance.

Disclosure Statement

The authors have no conflict of interest to declare.

References

1 Heng HH, Bremer SW, Stevens JB *et al.* Genetic and epigenetic heterogeneity in cancer: a genome-centric perspective. *J Cell Physiol* 2009; **220**: 538–47.
2 Hayden E. Cancer complexity slows quest for cure. *Nature* 2006; **455**: 148.
3 Grizzi F, Dileva A, Russo C *et al.* Cancer initiation and progression: an unsimplifiable complexity. *Theor Biol Med Model* 2006; **3**: 37.
4 Koenders PG, Peters WH, Wobbes T *et al.* Epidermal growth factor receptor levels are lower in carcinomatous than in normal colorectal tissue. *Br J Cancer* 1992; **65**: 189–92.
5 Messersmith W, Oppenheimer D, Peralba J *et al.* Assessment of epidermal growth factor receptor (EGFR) signaling in paired colorectal cancer and normal colon tissue samples using computer-aided immunohistochemical analysis. *Cancer Biol Ther* 2005; **4**: 1381–6.
6 Keshava Prasad TS, Goel R, Kandasamy K *et al.* Human protein reference database: 2009 update. *Nucleic Acids Res* 2009; **37**: D767–72.
7 Berthiaume JM, Wallace KB. Adriamycin-induced oxidative mitochondrial cardiotoxicity. *Cell Biol Toxicol* 2007; **23**: 15–25.
8 Imai K, Takaoka A. Comparing antibody and small-molecule therapies for cancer. *Nat Rev Cancer* 2006; **6**: 714–27.
9 Ricart AD, Tolcher AW. Technology insight: cytotoxic drug immunoconjugates for cancer therapy. *Nat Clin Pract Oncol* 2007; **4**: 245–55.
10 Matsumura Y, Maeda H. A new concept for macromolecular therapeutics in cancer chemotherapy: mechanism of tumoritropic accumulation of proteins and the antitumor agent smancs. *Cancer Res* 1986; **46**: 6387–92.
11 Matsumura Y. Poly (amino acid) micelle nanocarriers in preclinical and clinical studies. *Adv Drug Deliv Rev* 2008; **22**: 899–914.
12 Duncan R. Polymer conjugates as anticancer nanomedicines. *Nat Rev Cancer* 2006; **6**: 688–701.
13 Dvorak HF. Tumors: wounds that do not heal. Similarities between tumor stroma generation and wound healing. *N Engl J Med* 1986; **315**: 1650–9.
14 Ghajar CM, Bissell MJ. Extracellular matrix control of mammary gland morphogenesis and tumorigenesis: insights from imaging. *Histochem Cell Biol* 2008; **130**: 1105–18.
15 Minchinton AI, Tannock IF. Drug penetration in solid tumors. *Nat Rev Cancer* 2006; **6**: 583–92.
16 Trédan O, Galmarini CM, Patel K, Tannock IF. Drug resistance and the solid tumor microenvironment. *J Natl Cancer Inst* 2007; **99**: 1441–54.
17 Varki A. Trousseau's syndrome: multiple definitions and multiple mechanisms. *Blood* 2007; **110**: 1723–9.
18 Shoji M, Hancock WW, Abe K, Micko C. Activation of coagulation and angiogenesis in cancer: immunohistochemical localization *in situ* of clotting proteins and vascular endothelial growth factor in human cancer. *Am J Pathol* 1998; **152**: 399–411.
19 Stein PD, Beemath A, Meyers FA, Skaf E. Incidence of venous thromboembolism in patients hospitalized with cancer. *Am J Med* 2006; **119**: 60–8.
20 Belting M, Ahamed J, Ruf W. Signaling of the tissue factor coagulation pathway in angiogenesis and cancer. *Arterioscler Thromb Vasc Biol* 2005; **25**: 1545–50.
21 Hirakawa S, Kodama S, Kunstfeld R *et al.* VEGF-A induces tumor and sentinel lymph node lymphangiogenesis and promotes lymphatic metastasis. *J Exp Med* 2005; **201**: 1089–99.
22 Filler RB, Roberts SJ, Girardi M. Cutaneous two-stage chemical carcinogenesis. *CSH Protoc* 2007; **2007**: doi:10.1101/pdb.prot4837.
23 Lin KY, Maricevich M, Bardeesy N *et al. In vivo* quantitative microvasculature phenotype imaging of healthy and malignant tissues using a fiber-optic confocal laser microprobe. *Transl Oncol* 2008; **1**: 84–94.
24 Ellis LM, Fidler IJ. Finding the tumor copycat. Therapy fails, patients don't. *Nat Med* 2010; **16**: 974–5.
25 Hawighorst T, Velasco P, Streit M *et al.* Thrombospondin-2 plays a protective role in multistep carcinogenesis: a novel host anti-tumor defense mechanism. *EMBO J* 2001; **20**: 2631–40.

26 Doronina SO, Toki BE, Torgov MY *et al.* Development of potent monoclonal antibody auristatin conjugates for cancer therapy. *Nat Biotechnol* 2003; **21**: 778–84.
27 Wu AM, Senter PD. Arming antibodies: prospects and challenges for immunoconjugates. *Nat Biotechnol* 2005; **23**: 1137–46.
28 Lewis Phillips GD, Li G, Dugger DL *et al.* Targeting HER2-positive breast cancer with trastuzumab-DM1, an antibody-cytotoxic drug conjugate. *Cancer Res* 2008; **68**: 9280–90.
29 Koizumi F, Kitagawa M, Negishi T *et al.* Novel SN-38-incorporating polymeric micelles, NK012, eradicate vascular endothelial growth factor-secreting bulky tumors. *Cancer Res* 2006; **66**: 10.
30 Hamaguchi T, Doi T, Eguchi-Nakajima T *et al.* Phase I study of NK012, a novel SN-38-incorporating micellar nanoparticle, in adult patients with solid tumors. *Clin Cancer Res* 2010; **16**: 5058–66.
31 Bhowmick NA, Neilson EG, Moses HL. Stromal fibroblast in cancer initiation and progression. *Nature* 2004; **432**: 332–7.
32 Alderton GK. Tumor microenvironment: macrophages lead the way. *Nat Rev Cancer* 2010; **10**: 162–3.
33 Mosesson MW. Fibrinogen and fibrin structure and functions. *J Thromb Haemost* 2005; **3**: 1894–904.
34 Rehlaender BN, Cho MJ. Antibodies as carrier proteins. *Pharm Res* 1998; **15**: 1652–6.
35 Pommier Y. Topoisomerase I inhibitors: camptothecins and beyond. *Nat Rev Cancer* 2006; **6**: 789–802.
36 Bale WF, Spar IL, Goodland RL. Experimental radiation therapy of tumors with I^{131}-carrying antibodies to fibrin. *Cancer Res* 1960; **20**: 1488–94.
37 Finbloom DS, Magilavy DB, Harford JB, Rifai A, Plotz PH. Influence of antigen on immune complex behavior in mice. *J Clin Invest* 1981; **68**: 214–24.

Supporting Information

Additional Supporting Information may be found in the online version of this article:

Data S1. Detailed information regarding the synthesis of branched linker, branched PEG-linked SN-38, and NMR spectra for each compound.

Please note: Wiley-Blackwell are not responsible for the content or functionality of any supporting materials supplied by the authors. Any queries (other than missing material) should be directed to the corresponding author for the article.

doi: 10.1111/j.1349-7006.2011.01954.x

Bioconjugate Chemistry

ARTICLE

pubs.acs.org/bc

Cancer-Stroma Targeting Therapy by Cytotoxic Immunoconjugate Bound to the Collagen 4 Network in the Tumor Tissue

Masahiro Yasunaga,[†] Shino Manabe,[‡] David Tarin,[§] and Yasuhiro Matsumura*[,†]

[†]Investigative Treatment Division, Research Center for Innovative Oncology, National Cancer Center Hospital East, 6-5-1 Kashiwanoha, Kashiwa, Chiba, 277-8577, Japan

[‡]Synthetic Cellular Chemistry Laboratory, RIKEN Advanced Science Institute, 2-1 Hirosawa, Wako, Saitama 351-0198, Japan

[§]Department of Pathology and Moores/UCSD Comprehensive Cancer Center, University of California, San Diego, 3855 Health Sciences Drive MC 0803, La Jolla, California, 92093-0803, United States

ABSTRACT: Some cytotoxic immunoconjugates have been approved for malignant lymphoma, a representative of hypervascular and stroma-poor tumors. However, many human solid tumors possess abundant intercellular stromata that prevent diffusion of cancer cell-specific monoclonal antibodies (mAb) and become a barrier preventing immunoconjugates from directly attacking cancer cells. Here we show the successful development of a new strategy that overcomes this drawback and achieves a highly localized concentration of a topoisomerase I inhibitor, SN 38, by conjugating it via an ester bond to a mAb targeted against collagen 4, a plentiful component of the tumor stroma. Poly(ethylene glycol) (PEG) was utilized as a spacer, close to each bond, to maintain stability in the blood. Immunoconjugates selectively extravasated from leaky tumor vessels and minimally from normal vessels because the immunoconjugates are too large to pass through normal vessel walls. Stroma-targeting immunconjugates bound to the stroma to create a scaffold, from which sustained release of cytotoxic agent occurred and the agent subsequently diffused throughout the tumor tissue to damage both tumor cells and vessels. Cancer-stroma-targeting immunoconjugate therapy was thus validated as a new modality of oncological therapy, especially for refractory, stromal-rich cancers.

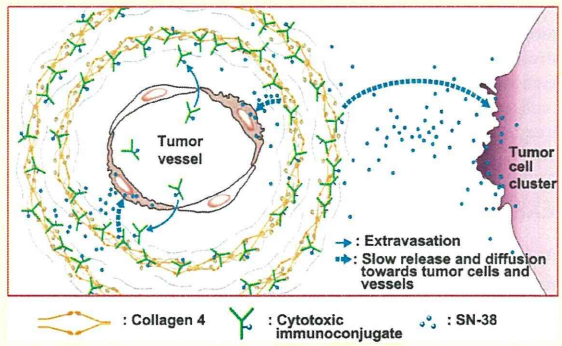

INTRODUCTION

In contrast to low molecular weight (LMW) agents, high molecular weight (HMW) agents such as monoclonal antibodies (mAbs) and nanoparticles have a long plasma half-life because they are too large to pass through the normal vessel walls, unless they are trapped by the reticuloendothelial system (RES) in various organs., However, HMW agents can reach tumor tissue sufficiently and extravasate efficiently from leaky tumor vessels to achieve tumor-selective accumulation of HMW agents by utilizing the enhanced permeability and retention (EPR) effect.[1−6] Even so, the use of HMW agents presents a dilemma for cancer therapy because the very properties that favor their high accumulation in the lesion also cause low diffusion of these macromolecules within a tumor.[7] Most human solid tumors possess abundant stromata that prevent mAb diffusion and, consequently, become a barrier preventing mAb from directly attacking cancer cells.[7−10] In fact, immunoconjugate therapies for common solid tumors (e.g., colorectal, lung, and pancreatic cancers) have not yet proven successful in clinical practice because of the heterogeneity of target antigens and the low uptake and retention of chemotherapeutic drugs in these types of cancer. This contrasts with the results seen in treatment of human hematologic malignancies and of tumor xenografts in mice, which usually have less inert interstitial tissue within the neoplasm.[11] The kinetics of drug distribution within tumors are considered to be functions of interstitial conductivity, which is determined by the quantity and density of the extracellular matrix (ECM e.g., proteoglycan, fibronectin), and fibrosis (e.g., collagen fibers) in the stroma.[7−10] Such compact assemblies of various tissue constituents in solid tumors cause reduced drug penetration and also act as a stromal barrier to prevent the diffusion of mAbs (HMW proteins).[7−9,11−13] Although there are a few papers describing tumor stromal targeting using immunoconjugates, the target molecule was still a surface antigen on cells in tumor stroma, or the ECM was used for targeting the tumor vascular endothelial cell.[14,15] The principle of our strategy is that our newly developed immunoconjugates selectively extravasated from leaky tumor vessels, bound to the collagen network in the stroma, and created a scaffold from which effective sustained release of the time-dependent ACA SN-38 occurred. This free SN-38 can easily reach the cancer cells by diffusion through the stromal barrier. Another important finding is that SN-38 released from immunoconjugates can attack and destroy the vascular endothelial cells (Figure1).

Received: March 29, 2011
Revised: June 30, 2011
Published: July 13, 2011

dx.doi.org/10.1021/bc200158j | *Bioconjugate Chem.* 2011, 22, 1776–1783

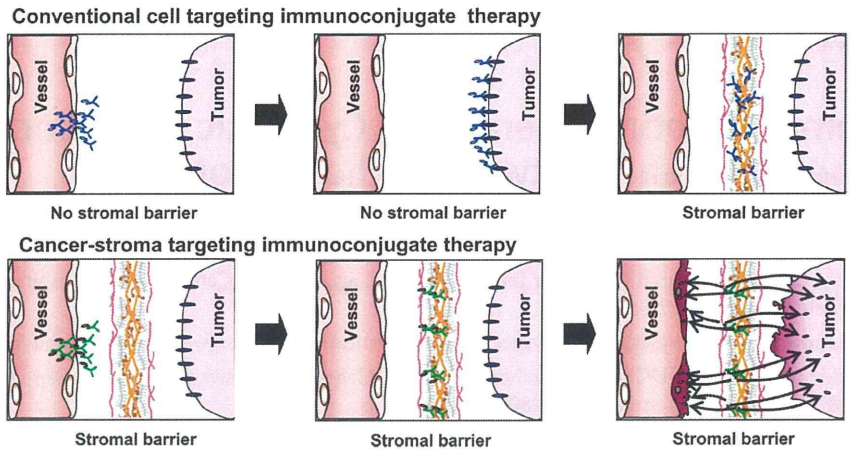

Figure 1. Therapeutic strategy of cancer-stroma targeting immunoconjugate. Conventional immunoconjugates can target cancer cells in the treatment of stroma-poor cancer such as malignant lymphoma. However, Many human solid tumors possess abundant stromata hindering the distribution of the immunoconjugates against cancer cells themselves (stromal barrier), whereas newly developed cancer-stroma-targeting immunoconjugates bound to the collagen 4 network of the cancer stroma, from which effective sustained release of the time-dependent anticancer agent SN-38 occurred. The SN-38 subsequently diffused throughout the tumor tissue to damage both cancer cells and vessels. Arrows show the distribution of SN-38 beyond the stromal barrier.

EXPERIMENTAL PROCEDURES

Antibody/Drug, Reagents, and Cells. Anti-EpCAM antibody-producing hybridoma (B8-4) was established from a mouse with immunizing recombinant protein (R&D Systems, Minneapolis, MN, USA). Anti-collagen 4 antibody-producing hybridoma (35-4) was obtained from a rat by immunization with purified mouse collagen 4 protein. A carrier protein was not used in either case.[16,17] Spleen cells from each immunized animal were fused with myeloma cells (P3X63Ag8.653). The specific hybridoma clones were selected using ELISA. Our anticollagen 4 antibody (35-4) was specific for mouse protein but not for human (data not shown). Antihuman CD20 antibody (rituximab) was purchased from Daiichi-Sankyo (Tokyo, Japan). For immunohistochemistry, polyclonal anti-collagen 4 antibody (LSL-LB-1403), monoclonal anti-CD31 antibody (MEC 13.3) and polyclonal anti-CD31 antibody (AF3628) were purchased from Cosmo. Bio. Inc. (Tokyo, Japan), Becton, Dickinson and Company (Franklin Lakes, NJ, USA), and R&D Systems, Inc. (Minneapolis, MN USA), respectively. SN-38 and CPT-11 (irinotecan) were purchased from Tokyo Chemical Industry Co. (Tokyo, Japan) and Yakult (Tokyo, Japan), respectively. Human pancreatic cancer cell line, PSN1 was purchased from the American Type Culture Collection (Rockville, MD, USA). Human pancreatic cancer cell line SUIT2 was purchased from the Health Science Research Resources Bank (Osaka, Japan). PSN1 and SUIT2 were maintained in DMEM (Sigma) supplemented with 10% fetal bovine serum (Tissue Culture Biologicals, CA, USA), penicillin, streptomycin, and amphotericin B (Sigma) in an atmosphere of 5% CO_2 at 37 °C. RL was maintained in RPMI1690 (Sigma) instead of DMEM.

Antibody Conjugate. A linker containing an ester bond between PEG and SN-38 was produced as follows. To a solution of SN-38 (102.1 mg, 0.260 mmol), BocHN-PEG_{27}-COOH (407.1 mg, 0.286 mmol) and 4-dimethylamino pyridine (15.9 mg, 0.130 mmol) in DMF (1 mL), 1-ethyl-3-(3-dimethyl aminopropyl)-carbodiimide·HCl (54.8 mg, 0.286 mmol) was added at 0 °C. The mixture was stirred at room temperature for 19 h, and the reaction mixture was purified by gel filtration column chromatography (LH20 $CHCl_3$/MeOH 1:1) and then silica gel column chromatography ($CHCl_3$/MeOH 15:1−9:1) to give the ester (420.1 mg, 90%) as a colorless oil.

^{1}H NMR (CD_3OD) δ 8.20 (d, J = 9.2 Hz, 1H), 7.99 (s, 1H), 7.66 (m, 2H), 5.60 (d, J = 16.5 Hz, 1H), 5.40 (d, J = 16.5 Hz, 1H), 5.32 (m, 2H), 3.93 (t, J = 6.4 Hz, 2H), 2.96 (t, J = 6.4 Hz, 2H), 1.97 (m, 2H), 1.43 (s, 9H), 1.40 (t, J = 7.6 Hz, 3H), 1,02 (t, J = 7.8 Hz, 3H); ^{13}C NMR (DMSO-d_6) δ 164.8, 161.9, 149.2, 148.5, 143.1, 142.7, 141.3, 138.2, 137.7, 137.5, 122.4, 119.5, 118.9, 117.2, 110.7, 106.5, 89.7, 70.4, 64.6, 62.3, 62.0, 62.0, 62.0, 61.9, 61.8, 61.8, 61.7, 61.5, 58.1, 58.0, 57.1, 41.2, 40.1, 31.8, 28.1, 26.3, 19.4, 14.4, 4.9, −1.1.

To a solution of BocHN-PEG_{27}-SN-38 (221.5 mg, 0.123 mmol) in CH_2Cl_2 (10 mL), trifluoroacetic acid (1 mL) was added at room temperature. After the mixture was stirred for 1.5 h, the solvent was removed in vacuo, and toluene was added. After evaporation, the residue was dried under high vacuum. The residue was dissolved in CH_2Cl_2 (5 mL) and MAL-PEG_{12}-NHS (128.2 mg, 0.148 mmol) and iPr_2NEt (48 μL, 0.246 mmol) were added at 0 °C. After 30 min, the mixture was purified by gel filtration column chromatography (LH-20, $CHCl_3$/CH_3OH = 1:1) and silica gel column chromatography to give (276.0 mg, 91%) of the target product as a colorless oil.

^{1}H NMR (CD_3OD) δ 8.20 (d, J = 9.2 Hz, 1H), 8.00 (s, 1H), 7.66−7.64 (m, 2H), 6.83 (s, 2H), 5.60 (d, J = 16.0 Hz, 1H), 5.41 (d, J = 16.0 Hz, 1H), 5.34 (s, 1H), 3.93 (t, J = 6.0 Hz, 2H), 2.97 (t, J = 6.0 Hz, 2H), 2.49−2.45 (m, 4H), 2.00−1.98 (m, 2H), 1.41 (t, J = 7.6 Hz, 3H), 1.02 (t, J = 7.6 Hz, 3H); ^{13}C NMR (DMSO-d_6) δ 172.1, 170.4, 169.8, 169.7, 169.1, 156.5, 151.7, 149.7, 148.9, 146.2, 145.6, 145.0, 134.3, 131.1, 128.4, 126.8, 125.3, 118.8, 115.0, 96.5, 72.3, 69.9, 69.6, 69.5, 69.4, 69.0, 68.9, 66.7, 65.8, 65.1, 49.5, 36.0, 34.8, 34.1, 33.9, 31.6, 30.3, 25.4, 22.3, 13.9, 7.8.

Interchain disulfides of the antibodies were first reduced with 10 mM DTT (Sigma).[18] The numbers of free thiols were quantified with dinitrothiocyanobenzene (DNTB, Wako). After the purification by gel filtration (Amicon Ultra Centrifugal Filter Devices, Millipore, Billerica, MA, USA), reduced antibodies

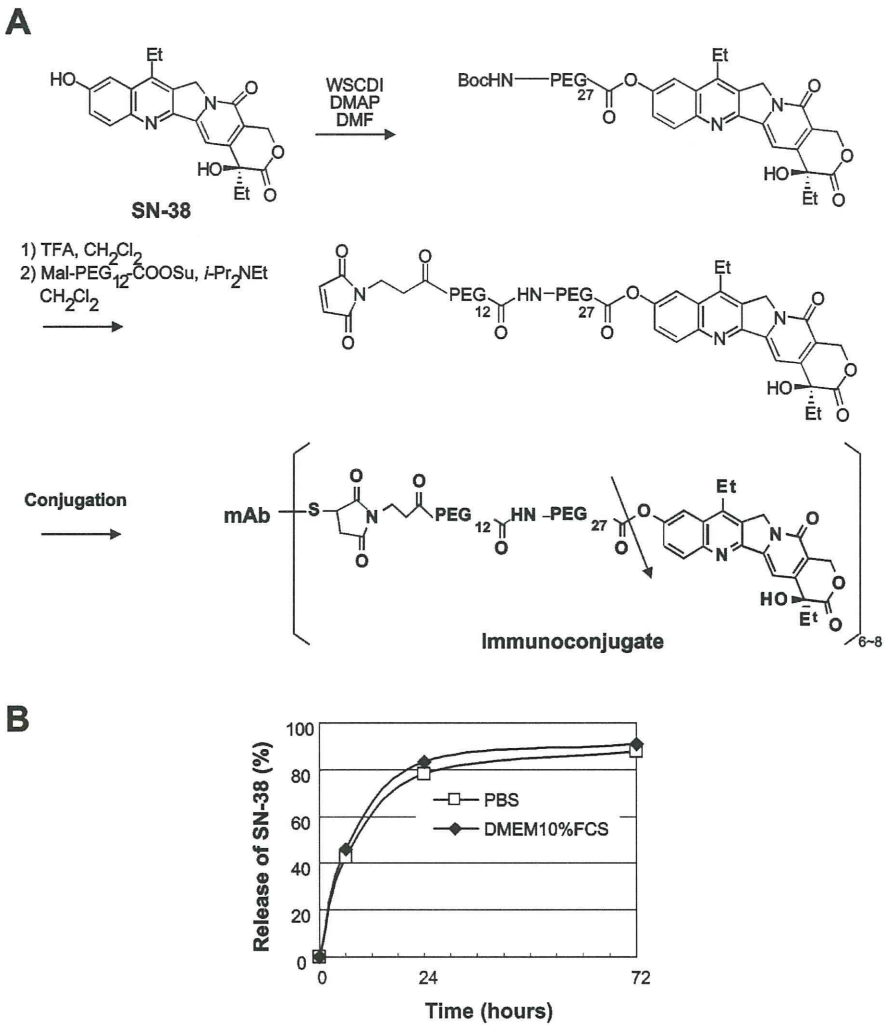

Figure 2. Structure and drug-release of the immunoconjugate. (A) Synthetic scheme of the immunoconjugate. The arrow indicates the cleavage site for releasing free active SN-38. PEG = poly(ethylene glycol). (B) The release behavior (nonenzymatic hydrolysis) of SN-38 from of the immunoconjugates.

(3.3 μM) were reacted with the SN-38 prodrugs (13.2 × [number of free thiols] μM) in PBS containing 5 mM EDTA (pH 6) at room temperature for 1 h, then at 4 °C overnight. SN-38-conjugated antibodies were purified by gel filtration (Amicon Ultra Centrifugal Filter Devices, Millipore). The concentration of antibody–prodrug conjugates was determined using the Bradford method (Bio-Rad Protein Assay, 500-0006JA, Bio-Rad). The numbers of residual thiols were quantified with DNTP. Each drug (SN-38)/antibody ratio was determined by comparison between the numbers of free and residual thiols (range from 6.7 to 8.4, Figure 2). For the evaluation of the antibody–drug coupling, the amount of forcibly detached SN-38 from the immunoconjugate was evaluated using HPLC (see next section).

High-Performance Liquid Chromatography (HPLC). The release behavior (nonenzymatic hydrolysis) of SN-38 from the immunoconjugates was investigated in vitro at 37 °C in DMEM with 10% FCS or PBS (pH 7.4). In addition to these reaction solutions at 6, 24, and 72 h in vitro, plasma and tumors on days 1, 3, and 7 after immunoconjugate injection in animal models were obtained. Reaction solutions and plasma were mixed with 0.1 M HCl at 50% (w/w). Tumors were rinsed with physiological saline, mixed with 0.1 M glycine-HCl buffer (pH 3.0) in methanol at 5% (w/w), and homogenized. To detect free SN-38 in the plasma, samples (50 μL) were mixed with 20 μL of 1 mM phosphoric acid in methanol (1:1) and 100 μL of camptothecin as internal standard solution. To detect free SN-38 in the tumor, samples (100 μL) were mixed with 20 μL of 1 mM phosphoric acid in methanol (1:1), 40 μL of ultrapure water, and 60 μL of internal standard solution. The samples were vortexed vigorously for 10 s and filtered through Ultrafree-MC centrifugal filter devices (Millipore, Bedford, MA, USA). To detect bound SN-38 in the immunoconjugate product itself, plasma or tumor samples (20 μL of plasma, 100 μL of tumor) were diluted with 20 μL of methanol (50% [w/w]) and 20 μL of NaOH (0.7 M). The samples were incubated for 15 min at room temperature. After incubation, 20 μL of HCl (0.7 M) and 60 μL of internal standard solution were added to the samples, and then the hydrolysate was filtered. Reverse-phase high-performance liquid chromatography (HPLC) was conducted at 35 °C on a Mightysil RP-18 GP column (150 mm × 4.6 mm; Kanto

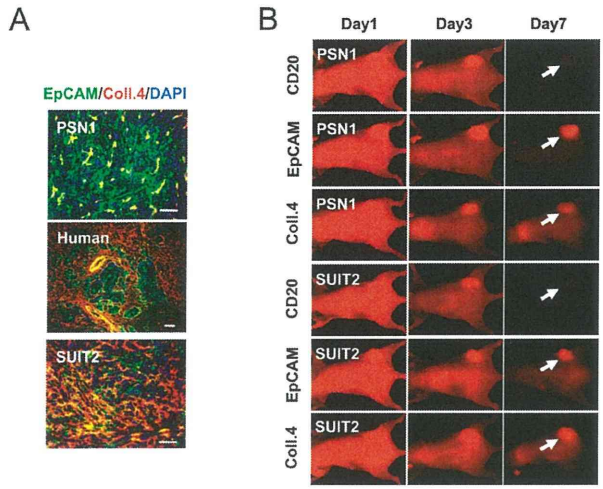

Figure 3. Intratumor accumulation of anti-EpCAM mAb and anti-collagen 4 mAb. (A) PSN1 and SUIT2 tumor and human pancreatic cancer were stained with anti-EpCAM (green), anticollagen 4 (red) mAb, and DAPI (blue). Scale bar = 100 μm. (B) In vivo imaging analysis of PSN1 and SUIT2 tumor was conducted using near-infrared labeled anti-CD20 (control), EpCAM, and collagen (coll.) 4 mAbs on days 1, 3, and 7 after injection. Arrows indicate each tumor position.

Chemical, Tokyo, Japan). The samples were injected into an Alliance Water 2795 HPLC system (Waters, Milford, MA, USA) equipped with a Waters 2475 multi-λ fluorescence detector. The detector was set at 365 and 540 nm (excitation and emission wavelengths, respectively) for SN-38.

In Vivo Imaging and Immunohistochemistry. Antibodies were conjugated with IRDye 800 (Li-Cor Biosciences, Lincoln, NE, USA) according to the manufacturer's protocol and injected to the tail vein at 100 μg. In vivo fluorescence imaging was performed by illuminating the animal using the OV110 small animal imaging system (Olympus Corp., Tokyo, Japan). Human specimens were purchased from US Biomax, Inc. (Rockville, MD, USA) and BioChain Institute, Inc. (Hayward, CA, USA). The tissues were incubated with anti-CD31 antibody (MEC 13.3 or AF3628), anti-collagen 4 antibody (35-4 or LSL-LB-1403), and anti-CD20 (rituximab) or anti-EpCAM antibody (B8-4) as first antibodies and Alexa 488- or 555-labeled anti-human, -mouse, -rat, or -goat IgG (Invitrogen) as second antibodies, respectively.

Animal Model and Antitumor Effects. Female BALB/c nude mice (5 weeks old) were purchased from SLC Japan (Shizuoka, Japan). Mice were inoculated subcutaneously in the flank with 2 $\times$ 10^6 cells of PSM1 and SUIT2. The length (L) and width (W) of tumor masses were measured every 4 days, and tumor volume was calculated using $(L \times W^2)/2$. All animal procedures were performed in compliance with the Guidelines for the Care and Use of Experimental Animals established by the Committee for Animal Experimental of the National Cancer Center. These guidelines meet the ethical standards required by law and also comply with the guidelines for the use of experimental animals in Japan. When the mean tumor volume reached approximately 90 mm^3 for PSM1 or approximately 70 mm^3 for SUIT2, mice were randomly divided into groups consisting of 5 mice each. Immunoconjugates were administered on day 0 by tail vein injection. The injection doses of antibody—SN-38 prodrug equal to an SN-38 dose of 3 mg/kg were determined by the calculation based on each drug (SN-38)/antibody ratio.

Statistical Analysis. Data were analyzed using ANOVA (Figure 4A,C) and Student's t test (Figure 4B). $P < 0.05$ was considered as significant.

RESULTS

Preparation of Cytotoxic Immunoconjugates. We developed two mAbs for tumor targeting, one against mouse collagen 4 abundantly found in the stroma of solid tumors, and another against human EpCAM which is strongly expressed in human cancer cells (Figure 3A). The third one was the mAb against CD20, which was used as a nonspecific control mAb for the human epithelial cancer cell lines. We used these three mAbs as vehicles to selectively exit the vascular system through the leaky tumor vessels and distribute within each tumor according to the nature of tumor stroma. Another special feature of our design was to conjugate highly cytotoxic SN-38 with each mAb using a specially selected linker, which provided both high serum stability and efficient, sustained drug release within the tumor lesion. SN-38 is a topoisomerase 1 inhibitor and an active component of CPT-11, which is used clinically for colorectal, lung, and other cancers. For the mAb conjugation to phenol—OH in SN-38, an ester bond was selected. In our design, poly(ethylene glycol) (PEG) was combined close to the bond mentioned above (Figure 2A). PEG is known to evade nonspecific capture by RES. The steric structure around the bond protects against immunoconjugate degradation in the blood. PEG has already been used for this purpose. [1−3,5,6] The drug (SN-38)/mAb ratio (the number of drugs attached to a mAb) of each immunoconjugate ranged from 6.7 to 8.4, which was calculated using DNTP method and validated by the evaluation of bound SN-38 in the conjugate using HPLC. Moreover, antigen recognition activity was estimated. In physiological conditions (nonenzymatic hydrolysis), the immunoconjugate can release SN-38 gradually and effectively (Figure 2B).

Intratumor Distribution of Anti-EpCAM mAb and Anti-collagen 4 mAb in Stroma-Poor or -Rich Tumors. We next clarified which types of xenograft tumors generated from human cell lines were stroma-rich or -poor. Immunohistochemistry using our 2 mAbs showed that tumors generated by the PSN1 cell line contained EpCAM-positive cells with interspersed collagen 4-positive stroma, different from that of freshly resected human pancreatic cancer (Figure 3A). On the other hand, SUIT2 tumor, reported as having histopathology relatively resembling the original human pancreatic cancer, [19,20] showed EpCAM-positive cells surrounded by a relatively high amount of collagen 4-positive stroma (Figure 3A). We then investigated the kinetics of entry of mAbs into the tumors using an in vivo imaging system with near-infrared fluorescence, which can provide deep tissue imaging with high fidelity. [21,22] Anti-CD20 mAb (rituximab), which is specific to human B cell lymphoma but not to carcinoma, was used as a nonspecific control because of its high specificity with less background. [11,23] Until day 3, all mAbs labeled with a near-infrared fluorescence dye including the control mAb were delivered to and retained in both PSN1 tumors, and SUIT2 tumors, indicating passive targeting by the EPR effect (Figure 3B). On day 7, anti-CD20 mAb was almost eliminated, but anti-EpCAM and anti-collagen 4 mAb were still retained in both types of tumors, indicating active targeting and retention, that is, binding to their respective ligands within the lesion.

dx.doi.org/10.1021/bc200158j |*Bioconjugate Chem.* 2011, 22, 1776–1783

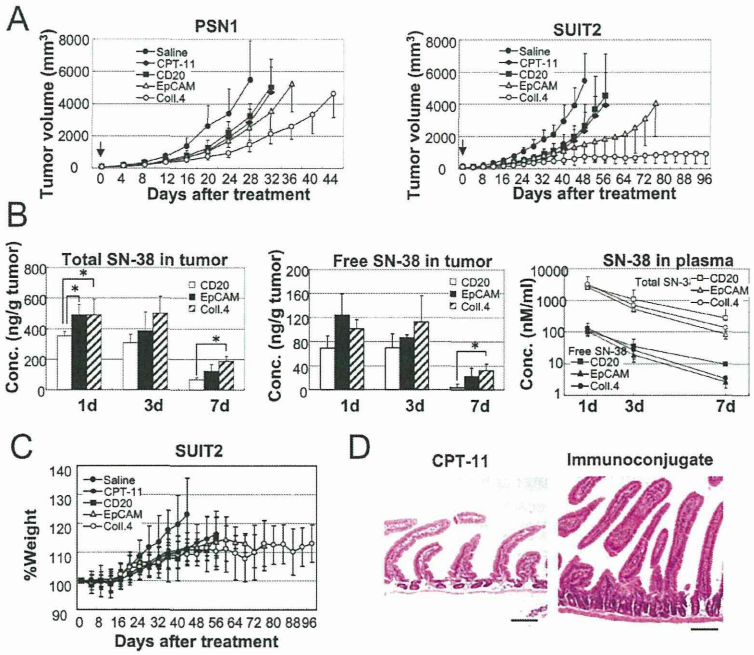

Figure 4. Antitumor effects, pharmacokinetics, and drug toxicities of anti-CD20, EpCAM, and collagen 4 immunoconjugates. (A) Antitumor activities in vivo were examined. In animal models of PSN1 and SUIT2, the three immunoconjugates or saline as control was administered to separate groups of mice by intravenous bolus injection on day 0. Arrows indicate day of administration, and the curves illustrate the effects of the treatments on tumor size. $P < 0.05$ (saline or CD20 vs EpCAM in PSN1), $P < 0.01$ (saline vs CPT11 or EpCAM in PSN1, CPT11 or CD20 vs EpCAM in SUIT2), $P < 0.001$ (saline vs CPT11 or CD20 or EpCAM in SUIT2, saline or CPT11 or CD20 or EpCAM vs collagen 4 in PSN1 or SUIT2). Bar = SD. (B) Tumor concentrations of total (bound and unbound) SN-38 (left) and free (unbound) SN-38 (center), and plasma concentrations (right) were determined using HPLC analysis. The concentrations on days 1, 3, and 7 are shown. * indicates $P < 0.05$; bar = SD. (C) Changes in the % body weight of saline, CPT-11, CD20, EpCAM, and collagen 4 in the same treated SUIT2 group (panel A). Bar = SD. (D) Pathologic mucosal change of jejunum from mouse treated with CPT11 (upper) or anti-collagen 4 immunoconjugate (lower). Scale bar = 1 mm. Coll.4, Collagen 4; Conc., concentration.

In addition there was a signal of near-infrared fluorescence at the area of lung after the treatment with anti-collagen 4 mAb (Figure 3B). We recognized same signals with some other commercially available antibodies such as anti-EGFR mAb. Although we have never observed lung toxicity in mice following administration of our immunoconjugate, we certainly need further investigation of this issue.

Antitumor Activity and Pharmacokinetic Studies in Stroma-Poor or -Rich Pancreatic Tumor Xenografts. Antitumor activities of immunoconjugates with ester bond SN-38 were evaluated in vivo. CPT-11 (clinically approved prodrug of SN-38, 66.7 mg/kg at maximum tolerance dose of this mouse, human clinical application is 100−750 mg/m^2)[24] and three immunoconjugates (administered once, at an equivalent SN-38 dose of 3 mg/kg; cytotoxic effect of SN-38 is 20 times more potent than CPT-11)[25,26] showed significant antitumor activities compared with results in mice treated with saline, in mice bearing either PSN1 (EpCAM-positive and stroma-poor) or SUIT2 (EpCAM-positive and stroma-rich) tumors. In SUIT2 tumors, while the tumor continued to increase in mice treated with CPT-11, anti-CD20 immunoconjugate, and anti-EpCAM immunoconjugate, the tumor treated in mice with anti-collagen 4 immunoconjugate stopped growing by about 1 month and never resumed up to 3 months (Figure 4A). In mice bearing PSN1 tumors (stroma poor), differences were present but less marked. Thus, anti-collagen 4−SN-38 immunoconjugate exerted the most potent antitumor activity compared with anti-CD20 or anti-EpCAM immunoconjugates and CPT-11, but the PSN1 tumor volume continued to increase slowly (Figure 4A). In both tumor models, anti-EpCAM immunoconjugate exerted superior antitumor effect compared with CPT-11 and anti-CD20 immunoconjugate, but inferior antitumor effect compared with anti-collagen 4 SN38-immunoconjugate.

A pharmacokinetic analysis in SUIT2-tumor bearing mice showed that the same high tumor concentrations of either free or total SN-38 (free and conjugated SN-38) were observed for all three immunoconjugates by day 3. On day 7, the tumor concentration of free and total SN-38 was scarcely detected in the tumor treated with anti-CD20 immunoconjugate (Figure 4B). On the other hand, significantly higher concentrations of free and total SN-38 were detected in tumor tissues of mice treated with the anti-collagen 4 immunoconjugate compared with the anti-CD20 immunoconjugate (Figure 4B). The tumor concentration of free and total SN-38 treated with anti-EpCAM immunoconjugate was intermediate among them, but not significant (Figure 4B). Regarding normal tissue distribution and elimination of antibodies and SN-38, there was no difference among immunoconjugates on day 7 after the administration. There was no significant difference in body weight changes among saline, CPT-11, and immunoconjugate groups (Figure 4C). In addition, there was no hepatotoxicity, nephrotoxicity, or bone marrow toxicity in mice treated with all three immunoconjugates compared with controls (data not shown). In the small intestinal mucosa of mice, widespread villous atrophy and decreased crypt density were observed during the treatment with free unbound CPT-11, which is well-known to have severe intestinal toxicity in

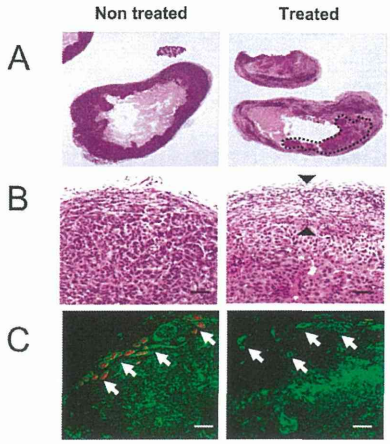

Figure 5. Histopathological features of SUIT2 tumors after anti-collagen 4 immunoconjugate treatment. (A) Hematoxylin and eosin staining of nontreated (left) and immunoconjugate-treated (right) SUIT2-tumors. A non-necrotic viable lesion in the treated tumor is enclosed by a dotted line. (B) The fibrotic capsule width in the treated tumor is indicated between black arrowheads. (C) Tumor vessels were examined by the CD31 (red)−collagen 4 (green) double-staining techniques. White arrows indicate tumor vessels or their traces in the boundary area. Scale bar = 100 μm.

clinics. On the other hand, the small intestinal mucosa of mice in groups treated with all immunoconjugates did not show any pathological change (Figure 4D).

Histopathological Features of SUIT2 Tumors after Anti-collagen 4 Immunoconjugate Treatment. The most important observation from a therapeutic standpoint was that only SUIT2 tumors treated with anti-collagen 4 immunoconjugate stopped growing about 1 month after treatment and remained dormant for more than 3 months. It is concluded that the strategy of orchestrating slow sustained release from a scaffold erected on the stable inert structural components of the tumor stroma is most effective. We compared histologically this nongrowing tumor with a size-matched, growing control tumor and found that both tumors showed central necrosis due to decreased blood flow, which is often observed in a murine xenotransplant model.[27,28] The striking difference was that large confluent necrotic zones and dense fibrotic capsule formation were observed only in the treated tumor (Figure 5A,B). In addition, CD31-positive endothelial cells, which may be tumor-feeding vessels in the peripheral part of the tumor, were never observed in the treated tumor compared with untreated control (Figure 5C). Instead, many collagen 4-positive round profiles corresponding to traces of destroyed vessels were observed in the peripheral area of the treated tumor (Figure 5C).

DISCUSSION

Cancer cells can acquire drug resistance via cellular and noncellular mechanisms.[7−9] The latter mechanisms involve various physiological barriers including excess interstitial stromal tissue, which prevents drug diffusion especially in human cancer.[7−10] Therefore, there is a rationale in overcoming this problem. In this study, we established two types of mAbs: anti-collagen 4 mAb for stroma targeting and anti-EpCAM mAb for tumor cell targeting. We then conjugated these mAbs with SN-38 using a newly designed linker assembly. Linker technology is an important part of immunoconjugate chemotherapy, and various linkers have been exploited to date. Among them, acid labile hydrazone linkage, thiol reduction of disulfide linkers, and enzymatic proteolysis of peptide linkers were favorably applied to ensure stability in plasma.[29,30] For these types of linkers, cell-mediated endocytosis and intracellular processing of the immunoconjugates were indispensable to make the active agent work. In our newly deployed linker construct, an ester bond was used for gradual cleavage in the extracellular space of the tumor. The interspaced PEG enables long survival of our immunoconjugates in the circulating plasma through a "stealth effect" permitting them to evade the RES. In addition, the immunoconjugates are too large to pass through the normal vessel wall, but they easily extravasate from leaky tumor vessels. Thus, our newly developed immunoconjugates can accumulate selectively in the tumor tissue and then exert sustained-release of SN-38. Our basic strategy for overcoming the stromal barrier as a protective shield for cancer cells is to make use of the stroma as a scaffold assembly of immunoconjugates, followed by the release of payload (anticancer agent) to the cancer cells. This free SN-38 can easily reach the cancer cells by diffusion, although the carrier mAb can hardly penetrate the stroma. Moreover, it was reported that collagen 4 in the outer layer of tumor vessels showed conspicuous structural abnormality and loose connection with both endothelial cells and pericytes, whereas that in normal tissue was well organized and tightly associated with the cells.[31] Therefore, SN-38-conjugated anti-collagen 4 mAb, which leaked out from tumor vasculature, can easily bind selectively to the collagen 4 matrix and accumulates within tumor tissues. It has been reported that tumor growth is angiogenesis-dependent and that tumors cannot grow if endothelial cell growth is limited. Moreover, there is evidence that accelerated tumor progression is only observed during the transition from the nonangiogenic stage to the angiogenic stage, a process termed "angiogenic switch".[32] Therefore, if this switch is turned off, tumors will stop growing and remain dormant indefinitely. Here, in our studies, only tumors treated with anti-collagen 4 mAb showed growth suppression and conversion to a dormant status, in keeping with reversal of the "switch". Our anti-collagen 4 immunoconjugate (mAb-bearing SN-38) can induce both tumor regression and the dormant state after a single, low-dose (SN-38, 3 mg/kg) injection. Interestingly, a dense fibrotic capsule was observed in the dormant tumor, which may be formed as a result of damage to the tumor vessels by released SN-38 and reaction of host defense in this lesion.

In our study, the antitumor activity of anti-EpCAM immunoconjugate was inferior to that of anti-collagen 4. We suggest that anti-EpCAM immunoconjugate may distribute unevenly within tumor cell areas and may possess less antivascular endothelial cell activity compared with anti-collagen 4 immunoconjugate.

The concentration of our immunoconjugate was much higher than that of trastuzumab−DM1 or other immunoconjugates used in previous studies.[33−35] The strategy of previous work was to reduce the dose of the mAb by selecting a very toxic agent and binding it to a mAb that can internalize into the tumor cells. Conversely, the principle of our strategy is that our immunoconjugate targets collagen 4 outside the tumor cells and allows the effective sustained release of SN-38 to attack tumor cells and vascular endothelial cells. The internalization ability of the antibody is irrelevant to our strategy. Therefore, in future we will have to exploit the linker to attach many drugs in combination with using a much more toxic agent like DM1 rather than SN-38

in order to reduce the administration dose of the antibody for clinical application.

There were a few papers describing tumor stromal targeting immunoconjugates, a mAb against a cell surface antigen FAP as fibroblast targeting therapy utilizing the internalization, or a mAb against fibronectin for the targeting of tumor vascular endothelial cells in photodynamic therapy.[14,15] In the latter, the drug directly damaged the stromal endothelial cells by the short and strong photochemical reaction. However, unlike those, our strategic concept is quite unique as follows:

(1) Newly developed SN-38-conjugated anti-collagen 4 Abs can extravasate from the leaky tumor vessels selectively and form a scaffold as it is captured by the collagen 4 network.

(2) The immunoconjugate allows the effective sustained release of SN-38 (a time-dependent anticancer agent) from the scaffold, and this released anticancer agent is distributed throughout the tumor.

(3) Consequently, the strategy described above was highly effective in causing arrest of tumor growth due to induced damage to tumor cells and tumor vessels without exerting adverse drug effects.The present method can be applied to other anticancer agents including molecular targeting agents by minor modification of chemical bonding between PEG and the drugs.

AUTHOR INFORMATION

Corresponding Author

*E-mail: yhmatsum@east.ncc.go.jp. Telephone and fax number: +81-4-7134-6857.

Notes

The authors declare that they have no conflict of interest.

ACKNOWLEDGMENT

This work was supported by Funding Program for World-Leading Innovative R&D on Science and Technology (FIRST Program) (Y.M.), Third Term Comprehensive Control Research for Cancer from the Ministry of Health, Labour and Welfare of Japan (Y.M.), a Grant-in-Aid for Scientific Research on Priority Areas from the Ministry of Education, Culture, Sports, Science and Technology, the Princess Takamatsu Cancer Research Fund (Y.M.), Japanese Foundation for Multidisciplinary Treatment of Cancer (Y.M.), Japanese Foundation for promotion of cancer research (M.Y.), and the Grant-in-Aid for Scientific Research from Japan Society for the Promotion of Science (M.Y.). We thank Dr. T. Sugino for his helpful discussion. We also thank Mrs. H. Koike and Miss M. Araake for their technical assistance and Mrs. K. Shiina for her secretarial support.

REFERENCES

(1) Peer, D., Karp, J. M., Hong, S., Farokhzad, O. C., Margalit, R., and Langer, R. (2007) Nanocarriers as an emerging platform for cancer therapy. *Nat. Nanotechnol. 2*, 751–760.

(2) Davis, M. E., Chen, Z. G., and Shin, D. M. (2008) Nanoparticle therapeutics: An emerging treatment modality for cancer. *Nat. Rev. Drug Discovery 7*, 771–782.

(3) Duncan, R. (2003) The dawning era of polymer therapeutics. *Nat. Rev. Drug Discovery 2*, 347–360.

(4) Matsumura, Y., and Maeda, H. (1986) A new concept for macromolecular therapeutics in cancer chemotherapy: mechanism of tumoritropic accumulation of proteins and the antitumor agent smancs. *Cancer Res. 46*, 6387–6392.

(5) Matsumura, Y. (2008) Poly(amino acid) micelle nanocarriers in preclinical and clinical studies. *Adv. Drug Delivery Rev. 22*, 899–914.

(6) Matsumura, Y., and Kataoka, K. (2009) Preclinical and clinical studies of anticancer agent-incorporating polymer micelles. *Cancer Sci. 100*, 572–579.

(7) Trédan, O., Galmarini, C. M., Patel, K., and Tannock, I. F. (2007) Drug resistance and the solid tumor microenvironment. *J. Natl. Cancer Inst. 99*, 1441–1454.

(8) Ghajar, C. M., and Bissell, M. J. (2008) Extracellular matrix control of mammary gland morphogenesis and tumorigenesis: insights from imaging. *Histochem. Cell Biol. 130*, 1105–1118.

(9) Minchinton, A. I., and Tannock, I. F. (2006) Drug penetration in solid tumors. *Nat. Rev. Cancer 6*, 583–592.

(10) Dvorak, H. F. (1986) Tumors: Wounds that do not heal. Similarities between tumor stroma generation and wound healing. *N. Engl. J. Med. 315*, 1650–1659.

(11) Ricart, A. D., and Tolcher, A. W. (2007) Technology insight: Cytotoxic drug immunoconjugates for cancer therapy. *Nat. Clin. Pract. Oncol. 4*, 245–255.

(12) Saito, Y., Yasunaga, M., Kuroda, J., Koga, Y., and Matsumura, Y. (2008) Enhanced distribution of NK012, a polymeric micelle-encapsulated SN-38, and sustained release of SN-38 within tumors can beat a hypovascular tumor. *Cancer Sci. 99*, 1258–1264.

(13) Mahadevan, D., and Von Hoff, D. D. (2007) Tumor-stroma interactions in pancreatic ductal adenocarcinoma. *Mol. Cancer Ther. 6*, 1186–1197.

(14) Ostermann, E., Garin-Chesa, P., Heider, K. H., Kalat, M., Lamche, H., Puri, C., Kerjaschki, D., Rettig, W. J., and Adolf, G. R. (2008) Effective immunoconjugate therapy in cancer models targeting a serine protease of tumor fibroblasts. *Clin. Cancer Res. 14*, 4584–4592.

(15) Palumbo, A., Hauler, F., Dziunycz, P., Schwager, K., Soltermann, A., Pretto, F., Alonso, C., Hofbauer, G. F., Boyle, R. W., and Neri, D. (2011) A chemically modified antibody mediates complete eradication of tumours by selective disruption of tumour blood vessels. *Br. J. Cancer 104*, 1106–1115.

(16) Herbert, W. J. (1978) Mineral-oil adjuvants and the immunisation of laboratory animals. *Handbook of Experimental Immunology*, 3rd ed (Weir, D. M., Ed.), pp A3.1−3.15, Blackwell, Oxford, U.K.

(17) Oi, V. T. Herzenberg, L. A. (1980) Immunoglobilin-producing hybrid cell lines.*Selected Methods in Cellular Immunology* (Misbell, B. B. Shiigi, S. M., Eds.). pp 351−372, WH Freeman & Co., New York.

(18) Sun, M. M., Beam, K. S., Cerveny, C. G., Hamblett, K. J., Blackmore, R. S., Torgov, M. Y., Handley, F. G., Ihle, N. C., Senter, P. D., and Alley, S. C. (2005) Reduction-alkylation strategies for the modification of specific monoclonal antibody disulfides. *Bioconjug Chem. 16*, 1282–1290.

(19) Iwamura, T., Katsuki, T., and Ide, K. (1987) Establishment and characterization of a human pancreatic cancer cell line (SUIT-2) producing carcinoembryonic antigen and carbohydrate antigen 19-9. *Jpn. J. Cancer Res. 78*, 54–62.

(20) Mauri, P., Scarpa, A., Nascimbeni, A. C., Benazzi, L., Parmagnani, E., Mafficini, A., Della Peruta, M., Bassi, C., Miyazaki, K., and Sorio, C. (2005) Identification of proteins released by pancreatic cancer cells by multidimensional protein identification technology: A strategy for identification of novel cancer markers. *FASEB J. 19*, 1125–1127.

(21) Folli, S., Westermann, P., Braichotte, D., Pèlegrin, A., Wagnières, G, van den Bergh, H, and Mach, J. P. (1994) Antibody-indocyanin conjugates for immunophotodetection of human squamous cell carcinoma in nude mice. *Cancer Res. 54*, 2643–2649.

(22) Mariani, G., Lasku, A., Balza, E., Gaggero, B., Motta, C., Di Luca, L., Dorcaratto, A., Viale, G. A., Neri, D., and Zardi, L. (1997) Tumor targeting potential of the monoclonal antibody BC-1 against oncofetal fibronectin in nude mice bearing human tumor implants. *Cancer 80*, 2378–2384.

(23) Armstrong, A., and Eck, S. L. (2003) EpCAM: A new therapeutic target for an old cancer antigen. *Cancer Biol. Ther. 2*, 320–326.